Technical Article

The Use of Cylinder Functions in the Solution of Electromagnetic Problems

***Abstract* — This article presents and gives examples of the use of toroidal harmonics for the expansion of the inverse distance in cylindrical coordinates. The article then shows its use in problems for structures that are generally finite cylinders. However the method is not limited to cylindrical or symmetric geometries. The method is well adapted to problems in which the far field is required and for problems where very smooth fields are needed.**

I. Introduction

It is well known that a Laplacian field can be expressed in terms of spherical or spheroidal harmonics [2, 20]. Expansions are also available in cylindrical coordinates for problems of infinite length. There has not been a convenient formulation for finite cylinders. This formulation has been very useful for the author in analysis of geometries such as electric machines, solenoids and other cylindrical devices. The formulation to be presented here also has the property that it provides, as in the case of the spherical harmonic expansion, a set of discrete sources similar and related to the familiar monopole, dipole, quadrupole series of spherical harmonics.

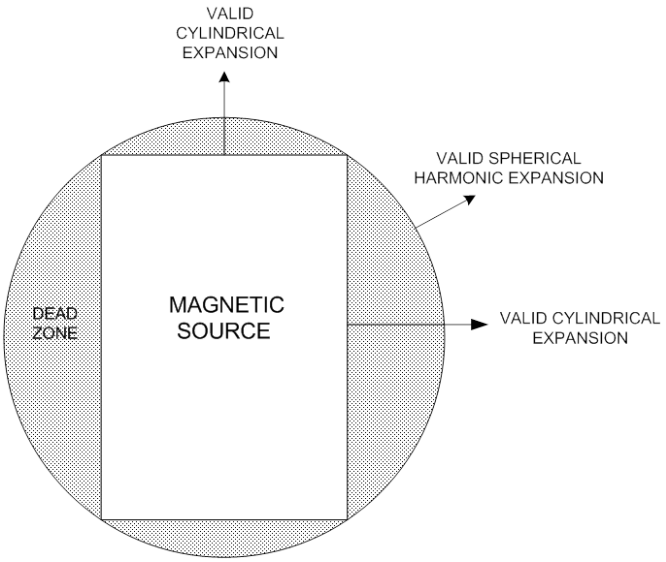

Figure 1: Domain of a problem showing a spherical and cylindrical bounding surface

The original problem that led to this development was a problem of electromagnetic compatibility. The leakage fields produced by an electromagnetic device (a permanent magnet motor in this case) were having an adverse effect on near-by electronics and sensors. In fact it was necessary to model the exterior fields to a distance of 10's of meters from the machine, even up to 100 diameters. The exterior fields were extremely small of course. We have shown [9, 10] that in almost all cases, the exterior field is dominated by asymmetries in the machine. Some of these asymmetries are part of the design, such as lead boxes and frames, and some are due to manufacturing tolerances and unbalanced magnets. Due the very small magnitude of the fields and the difficulty in making accurate measurements in what are usually noisy environments, the measurements are made as close as possible to the machine, which in this case has a roughly cylindrical shape.

To solve this problem we first performed a spherical multipole decomposition from a finite element solution. We found the potential or field on a sphere surrounding the source region. The multipole solution is only valid in the region exterior to the observation sphere and there is a large "dead zone" between the cylinder and the sphere for which we have no valid expansion. This is illustrated in Figure (1). The measurements, due to the low magnitude of the leakage field and the fact that the high order terms fall off very quickly, were made using a cylindrical array of magnetometers very close to the source. We therefore needed an expansion for a finite cylinder which would include the measurement points.

In a search of the literature, we could not find a formulation that had been applied to potential or field problems although the mathematics had been developed over a century before [4, 5, 6]. We have now applied this method to the problem described above and also to a number of other problems in potential theory [14, 15, 21]. We have also found that expansion in terms of zonal harmonics or cylinder functions has a number of very attractive numerical properties such as very fast convergence. It also was discovered by Selvaggi [14] that one can associate the different terms in the cylinder expansion with equivalent infinitesimal charge or pole distributions and that there is a relation between the terms in the cylindrical expansion and the familiar spherical harmonics.

II. Formulation

The expansion is found referring to Figure 2 which defines the coordinate system.

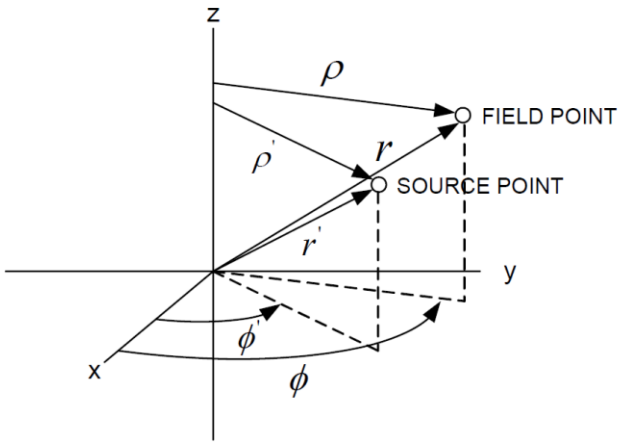

Figure 2: Cylindrical Coordinate System with Source and Observation Points

where the source coordinates are (ρ',ϕ',z') and the observation coordinates are (ρ,ϕ,z).

We now find an expression for the inverse distance in these coordinates. This is given in equation 1.

$$\frac{1}{|r-r'|}=\frac{1}{\sqrt{\rho^2+\rho'^2+(z-z')^2-2\rho\rho'\cos(\phi-\phi')}} \quad (1)$$

It is common to express the right hand side of (1) in terms of Bessel function so that [1,2]

For $\rho>\rho'$ we have

$$\frac{1}{|r-r'|}=\frac{2}{\pi}\sum_{m=-\infty}^{\infty}e^{jm(\phi-\phi')}\int_0^{\infty}K_m(\rho u)I_m(\rho' u)\cos[u(z-z')]du \quad (2)$$

And for $\rho'>\rho$ we have

$$\frac{1}{|r-r'|}=\frac{2}{\pi}\sum_{m=-\infty}^{\infty}e^{jm(\phi-\phi')}\int_0^{\infty}K_m(\rho' u)I_m(\rho u)\cos[u(z-z')]du \quad (3)$$

We can write this in a more compact for by defining

$$\Theta_m(\rho,\phi,z)=\int_0^{\infty}K_m(\rho u)I_m(\rho' u)\cos[u(z-z')]du \quad (4)$$

$$\Lambda_m(\rho,\varphi,z)=\int_0^{\infty}K_m(\rho' u)I_m(\rho u)\cos[u(z-z')]du \quad (5)$$

We now have for the two cases

$$\frac{1}{|r-r'|}=\frac{2}{\pi}\sum_{m=0}^{\infty}\varepsilon_m\Theta_m(\rho,\phi,z)\cos[m(\phi-\phi')] \quad (6)$$

and

$$\frac{1}{|r-r'|}=\frac{2}{\pi}\sum_{m=0}^{\infty}\varepsilon_m\Lambda_m(\rho,\phi,z)\cos[m(\phi-\phi')] \quad (7)$$

ε_m is [18] the Neumann factor which can be expressed in terms of the Kronecker Delta. This is represented by $\varepsilon_m=2-\delta_m^0$ where $\delta_m^0=1$ if $m=0$ and $\delta_m^0=2$ for $m\geq 1$.

The numerical solution of equation (4) or equation (5) requires the accurate evaluation of the infinite integral over a product of modified Bessel functions for all m. This has proven to be a rather difficult problem and it is one reason why equation (4) or equation (5) has not been extensively utilized. However, one can simplify these equations and eliminate the need for numerical integration.

It has been shown that [14]

$$\frac{1}{|r-r'|}=\frac{1}{\pi\sqrt{\rho\rho'}}\sum_{m=0}^{\infty}\varepsilon_m Q_{m-1/2}(\beta)\cos[m(\phi-\phi')] \quad (8)$$

where Q is called a Legendre function of the second kind and half-integral degree, or a toroidal function of zeroth order and of half-integral degree. They are also referred to as Q functions. Equation (8) represents a Fourier series expansion of the inverse distance function in cylindrical coordinates whose weighting coefficients are the toroidal functions. We can now express equations (4) and (5) as

$$\Theta_m(\rho,\phi,z)=\frac{1}{2\sqrt{\rho\rho'}}Q_{m-1/2}\left(\frac{\rho^2+\rho'^2+(z-z')^2}{2\rho\rho'}\right) \quad (9)$$

$$\Lambda_m(\rho,\phi,z)=\frac{1}{2\sqrt{\rho\rho'}}Q_{m-1/2}\left(\frac{\rho^2+\rho'^2+(z-z')^2}{2\rho\rho'}\right) \quad (10)$$

We note also that Θ_m and Λ_m are the same so we have only one expansion instead of the two for the Bessel functions which is a distinct advantage.

We can express the magnetic potential at a point, due to an array of magnetic charges, Ω_k as

$$\Phi_M(\rho,\phi,z)=\frac{1}{4\pi}\sum_{k=1}^{N}\frac{\Omega_k}{\sqrt{\rho^2+\rho_k^2+(z-z_k)^2-2\rho\rho_k\cos(m(\phi-\phi_k))}} \quad (11)$$

In terms of the toroidal harmonics we have

$$\Phi_M(\rho,\phi,z)=\frac{1}{4\pi^2}\sum_{k=1}^{N}\frac{\Omega_k}{\sqrt{\rho\rho_k}}\sum_{m=0}^{\infty}\varepsilon_m Q_{m-\frac{1}{2}}(\beta_k)\cos(m(\phi-\phi_k)) \quad (12)$$

where

$$\beta=\frac{\rho^2+\rho'^2+(z-z')^2}{2\rho\rho'}>1 \quad (13)$$

A. Derivatives

Very often it is necessary to take derivatives of the potential or the field. The derivatives of the toroidal functions (and integrals as well) are easily found in analytical form [14]. The field then is found as the gradient of the potential as described in equation (14). High order derivatives are also easily found analytically.

$$\nabla\left(\frac{1}{|r-r'|}\right)=\frac{1}{\pi}\sum_{m=0}^{\infty}\varepsilon_m\left(\frac{\partial}{\partial\rho}\left(\frac{Q_{m-\frac{1}{2}}(\beta)}{\sqrt{\rho\rho'}}\right)\cos[m(\phi-\phi')]\hat{\rho}+\frac{\partial}{\partial\phi}\left(\cos[m(\phi-\phi')]\right)\left(\frac{Q_{m-\frac{1}{2}}(\beta)}{\sqrt{\rho\rho'}}\right)\frac{\hat{\phi}}{\rho}+\frac{\partial}{\partial z}\left(Q_{m-\frac{1}{2}}(\beta)\right)\frac{\cos[m(\phi-\phi')]}{\sqrt{\rho\rho'}}\hat{z}\right) \quad (14)$$

III. EXAMPLES

To see some of the interesting properties of these functions let us consider the problem of a thin circular loop of current. This of course has a well-known solution [2, 16].

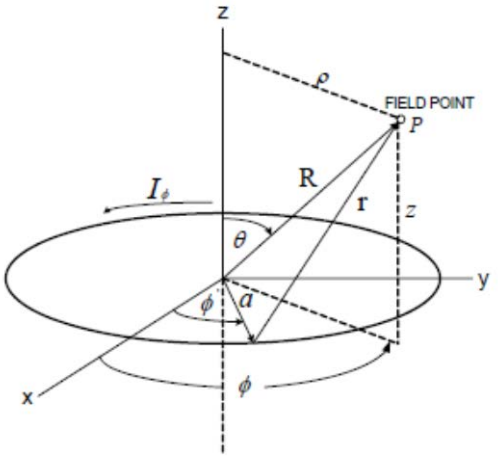

Figure 3: Current Loop in Cylindrical Coordinates

In terms of the Q functions the solution for the vector potential is [14]

$$A(\rho,z)=\frac{\mu_0 I_\phi}{2\pi}\sqrt{\frac{a}{\rho}}Q_{1/2}(\beta)\hat{\phi} \quad (15)$$

The evaluation of equation (15) requires no numerical integration, only a quickly converging summation for the $Q_{\frac{1}{2}}$.

A very interesting property of the toroidal harmonics is their relation to terms of a spherical harmonic expansion. The definition of the coordinates is illustrated in Figure 4.

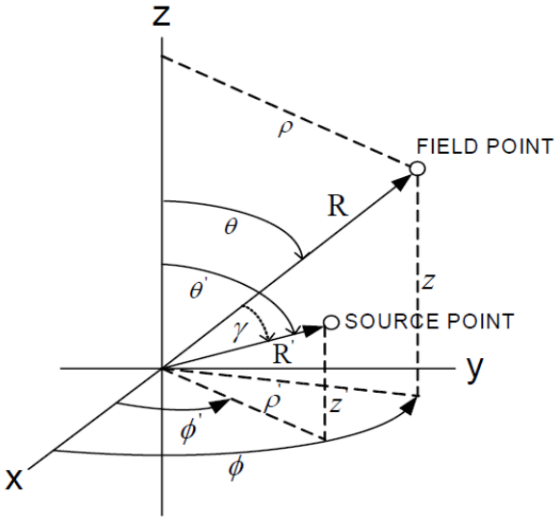

Figure 4: Definition of Spherical and Cylindrical Coordinates.

The expansion of the inverse distance in spherical coordinates yields the well-known multi-pole decomposition. The coefficients of the $\frac{1}{r^n}$ terms are Legendre or Associated Legendre polynomials. In terms of potential, we have the first term or monopole which falls off as $\frac{1}{r}$, then the dipole which falls off as $\frac{1}{r^2}$ and so forth.

Consider now the expansion for the first three Q functions.

$$\frac{1}{\pi\sqrt{\rho a}}Q_{-1/2}(\rho,z)=\frac{1}{\sqrt{R^2+a^2}}\times$$
$$\left(1+\frac{3}{4}\frac{R^2a^2\sin^2\theta}{\left(R^2+a^2\right)^2}+\frac{105}{64}\frac{R^4a^4\sin^4\theta}{\left(R^2+a^2\right)^4}+\cdots\right) \quad (16)$$

and

$$\frac{1}{\pi\sqrt{\rho a}}Q_{1/2}(\rho,z)=\frac{Ra\sin\theta}{2\left(R^2+a^2\right)^{3/2}}\times$$
$$\left(1+\frac{15}{8}\frac{R^2a^2\sin^2\theta}{\left(R^2+a^2\right)^2}+\frac{945}{192}\frac{R^4a^4\sin^4\theta}{\left(R^2+a^2\right)^4}+\cdots\right) \quad (17)$$

$$\frac{1}{\pi\sqrt{\rho a}}Q_{3/2}(\rho,z)=\frac{R^2a^2\sin^2\theta}{4\left(R^2+a^2\right)^{5/2}}\times$$
$$\left(\frac{3}{2}+\frac{105}{24}\frac{R^2a^2\sin^2\theta}{\left(R^2+a^2\right)^2}+\frac{3465}{256}\frac{R^4a^4\sin^4\theta}{\left(R^2+a^2\right)^4}+\cdots\right) \quad (18)$$

We see from equations (16), (17) and (18) that as *R* gets large, we obtain a series of discrete terms which have different $\frac{1}{r^n}$ terms. For example, considering the $Q_{-\frac{1}{2}}$ term, for large *R* we can find $\frac{1}{r}, \frac{1}{r^3}, \cdots$ terms, corresponding to the fall-off rate of the monopole, quadrupole, and higher terms. Referring to Table 1 below, we see that it is only the $Q_{-\frac{1}{2}}$ term that can contain a spherical monopole term. Similarly the $Q_{\frac{1}{2}}$ term is the only one which can have a spherical dipole or $\frac{1}{r^2}$ potential. Looking back now at equation (15) we see that as expected, the $Q_{\frac{1}{2}}$ solution for the loop of current contains the dipole term. The far field of the current loop thus looks like a spherical dipole. It is not the case that the second term corresponds directly to a dipole field. The term is richer in $\frac{1}{r^n}$ terms and reflects the cylindrical nature of the problem.

Note also that there are two different terms that contain the spherical quadrupole and octupole. Table 1 is quite useful in assigning different physical characteristics of the problem to the near and far field results.

$Q_{m-\frac{1}{2}}(\rho,z)$	*spherical* *monopole* 2^0	*spherical* *dipole* 2^1	*spherical* *quadrupole* 2^2	*spherical* *octupole* 2^3	*spherical* *hexadecapole* 2^4	$\cdots$
$\frac{1}{\pi\sqrt{\rho a}}Q_{-\frac{1}{2}}(\rho,z)$	×		×		×	
$\frac{1}{\pi\sqrt{\rho a}}Q_{\frac{1}{2}}(\rho,z)$		×		×		
$\frac{1}{\pi\sqrt{\rho a}}Q_{\frac{3}{2}}(\rho,z)$			×		×	
$\frac{1}{\pi\sqrt{\rho a}}Q_{\frac{5}{2}}(\rho,z)$				×		
$\frac{1}{\pi\sqrt{\rho a}}Q_{\frac{7}{2}}(\rho,z)$					×	
$\vdots$						$\ddots$

Table 1: Relation of Toroidal Functions and Spherical Harmonics

Another example of the use of these functions is illustrated in Figure 5. In this case we have a cylindrical magnet which is magnetized in a direction perpendicular to its axis. This was chosen since this example does not have cylindrical symmetry. Also there exists another analytical solution [8] requiring numerical integration which facilitated verifying the results.

In terms of toroidal functions we can write the solution for the magnetic scalar potential as [14]

$$\Phi_P = \frac{M_0}{4\pi^2}\sqrt{\frac{a}{\rho}}\sum_{m=0}^{\infty}\varepsilon_m \int_{-L}^{L}\int_{0}^{2\pi} Q_{m-\frac{1}{2}}(\beta)\times \cos\left[m(\phi-\varphi')\right]\cos(\phi')\,d\phi'\,dz' \quad (19)$$

The integrations can be done analytically and the solution is given in [14]. The solution is now in terms on an infinite summation of the Q functions.

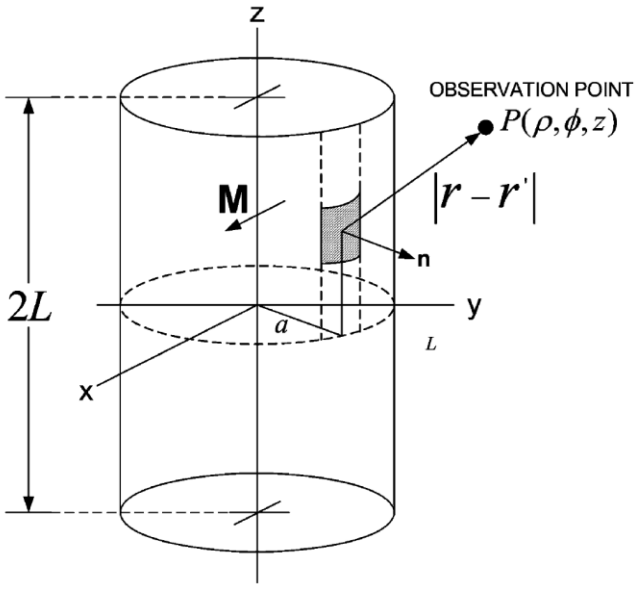

Figure 5: Cylindrical Magnet with Perpendicular Magnetization.

Figure (6) shows the radial flux density on the cylinder just from the first term of the expansion.

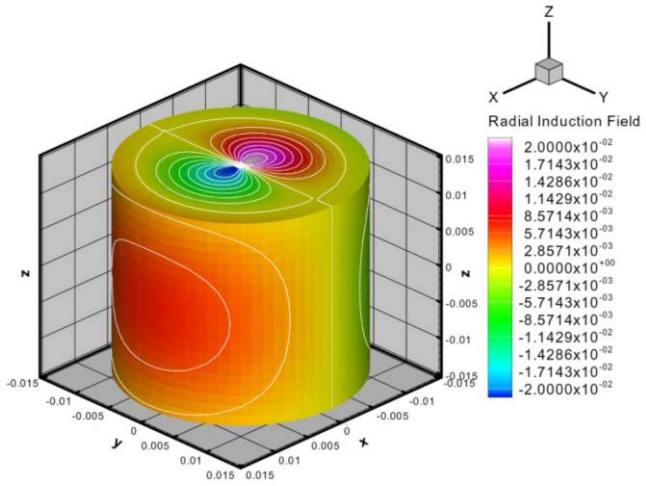

Figure 6: Radial Flux Density from One Term in the Expansion

Figure (7) shows the radial component of the flux density with the first 10 terms of the Q expansion. We see that the shapes or Figures (6) and (7) are quite similar and in fact the solution converges very quickly.

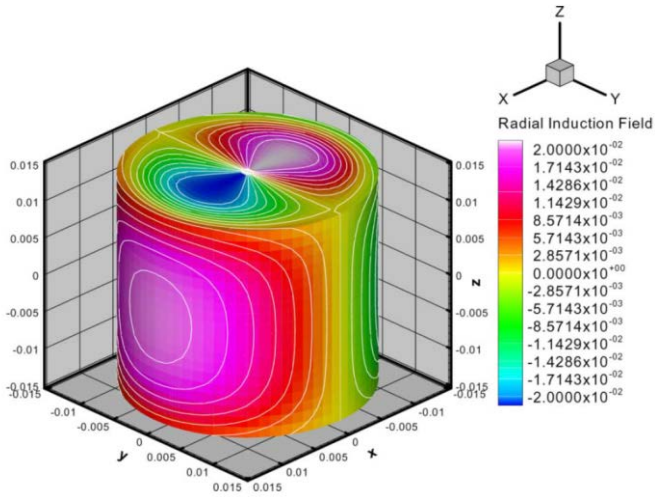

Figure 7: Radial Flux Density using 10 terms in the expansion

Figure (8) shows the axial component of the flux density for 10 terms in the series.

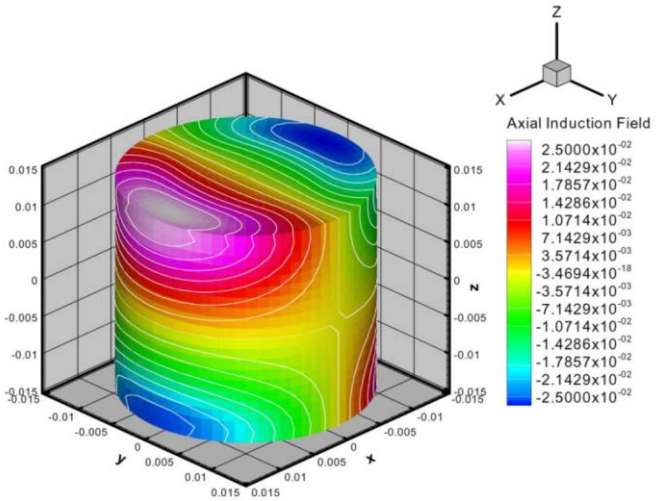

Figure 8: Axial Flux Density for the Cylindrical Magnet

We now return to the problem which led to the use of these special functions. Let us consider a six pole permanent magnet motor. This is a commercial motor for which we have the geometrical and materials data. The motor has 6 surface mounted radial magnets. The orientation of the magnets is shown in Figure (9).

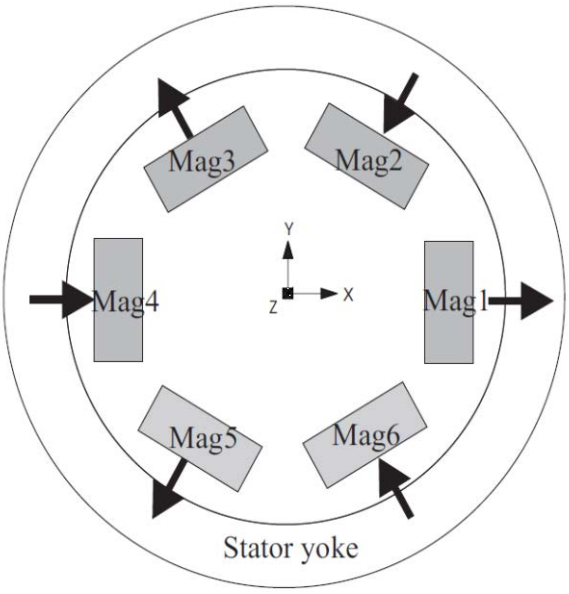

Figure 9: Magnet Arrangement for Six Pole Permanent Magnet Motor

A finite element solution was obtained for the machine in 3 dimensions. The outer layer of the machine showing the mesh is illustrated in Figure (10). A large region exterior to the motor was also modeled and the solution space was then terminated with an infinite box to simulate an open boundary.

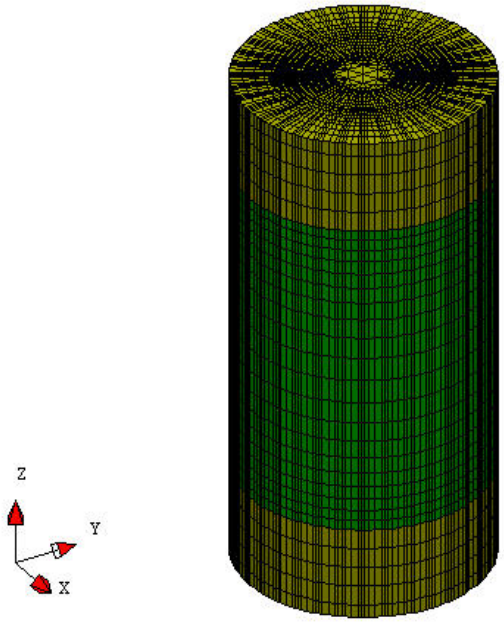

Figure 10: Finite element model of 6 pole permanent magnet motor

Several cases were considered. The first assumes that the motor is perfectly balanced with no asymmetries. We then added defects to the machine. In this case we added unbalanced magnets and an axial displacement between rotor and stator.

We first used a spherical multipole decomposition. One method of finding sources to get the coefficients of the spherical expansion is the well-known charge simulation method. From the finite element solution we get a set of potentials (or flux density) on a sphere surrounding (but not intersection) the motor. This is illustrated in Figure (11) in which we see the sphere with known potential and, internal to that sphere, a sphere with unknown magnetic equivalent charges. If we use the same number of unknown charges and observation points we obtain a square matrix as shown in equation (20). Once the unknown charges are found we use these to find the multipole decomposition which is valid only outside the potential sphere.

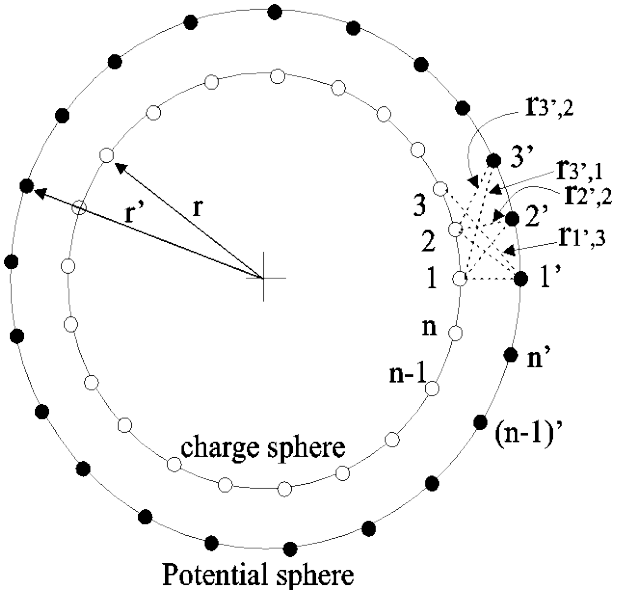

Figure 11: Sphere of Observation Points and Equivalent Magnetic Charges

$$\begin{bmatrix} \Omega_1 \\ \Omega_2 \\ \vdots \\ \Omega_n \end{bmatrix} = 4\pi \begin{bmatrix} \frac{1}{r_{11}} & \frac{1}{r_{12}} & \cdots & \frac{1}{r_{1n}} \\ \frac{1}{r_{21}} & \frac{1}{r_{22}} & \cdots & \frac{1}{r_{2n}} \\ \vdots & \vdots & \ddots & \vdots \\ \frac{1}{r_{n1}} & \frac{1}{r_{n2}} & \cdots & \frac{1}{r_{nn}} \end{bmatrix}^{-1} \begin{bmatrix} \Phi_1 \\ \Phi_2 \\ \vdots \\ \Phi_n \end{bmatrix} \quad (20)$$

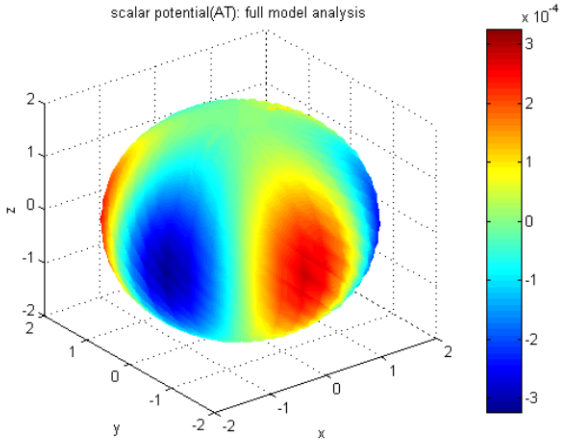

Figure 12: Scalar Potential on a Sphere Outside the Motor for Balaned Conditions

The plot in Figure (12) is of the scalar potential and shows the expected six pole distribution. In terms of spherical harmonics, the machine's dominant signature is the octupole. There are other multipole terms, but their contributions are very small outside the motor.

In Figure (13) we see only the octupole contribution to the total field. It is essentially the same as Figure (12).

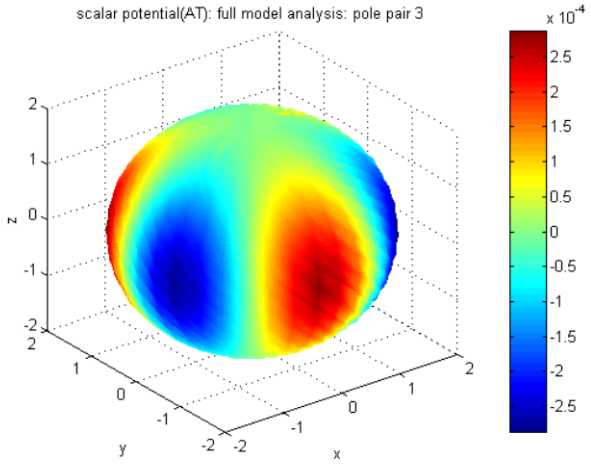

Figure 13: The Octupole Contribution to the Scalar Potential for the Balanced Condition

We now look at an unbalanced case. In Figure (14) we see the scalar potential on our observation sphere for the same motor but with one magnet slightly demagnetized. This small unbalance leads to the production of a dipole. The dipole strength is small but it persists longer in the far-field due to its slower decay rate. Even near the motor, the dipole overwhelms the main field (octupole) which is essentially unchanged from the balanced case. This can be seen by comparing Figure (15), which is the octupole component of the potential for the unbalanced magnet case, with Figure (13) for the balanced case.

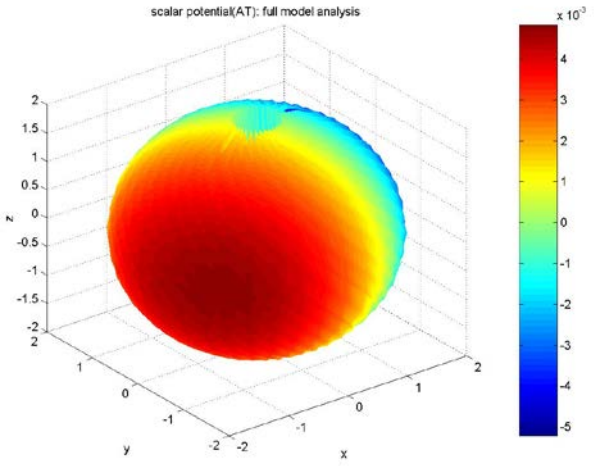

Figure 14: Scalar Potential for Unbalamced Case

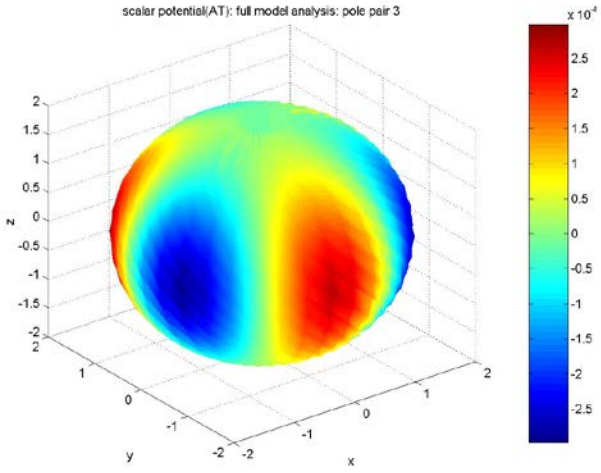

Figure 15: Octupole Component for the Unbalanced Case.

The spherical harmonic distribution works well and provides useful information. However, it does not provide a solution close the magnetic source. This is especially important in analyzing sources with large aspect ratios.

To overcome this limitation, we analyzed the same problem using the cylindrical functions. The same finite element solution is used. In this case we compute a magnetic scalar potential solution on a cylinder surrounding the object of interest. The solution is found on a finite set of observation points as shown in Figure (16). We then find a set of magnetic charges on another cylinder just inside the observation cylinder. These charges produce the same exterior field as the original problem just as in the case of the spherical harmonics. The advantage of having a finite number of charges is that it is relatively simple to find the multi-pole distribution (spherical) or the cylindrical distribution.

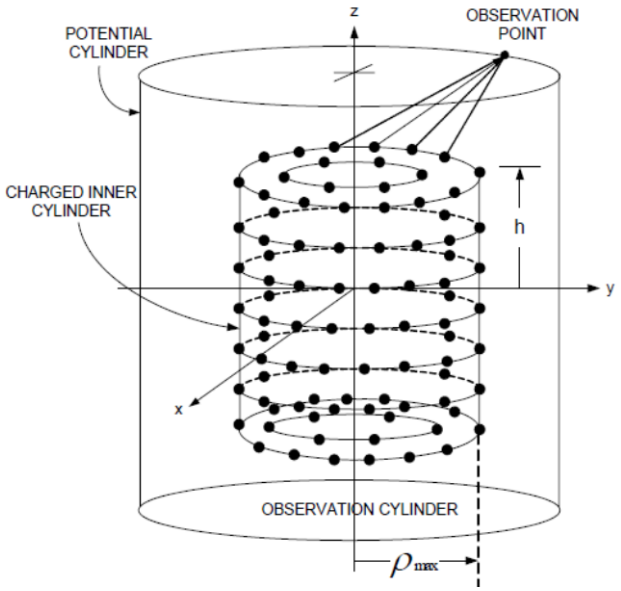

Figure 16: Potential Cylinder and Equivalent Magnetic Charges

.

Figure (17) shows the magnetic scalar potential on the observation cylinder for the case of the balanced magnets. We note again that for the balanced magnetic problem, the dominant component of the field is the six radial pole distribution which is clearly evident in Figure (17).

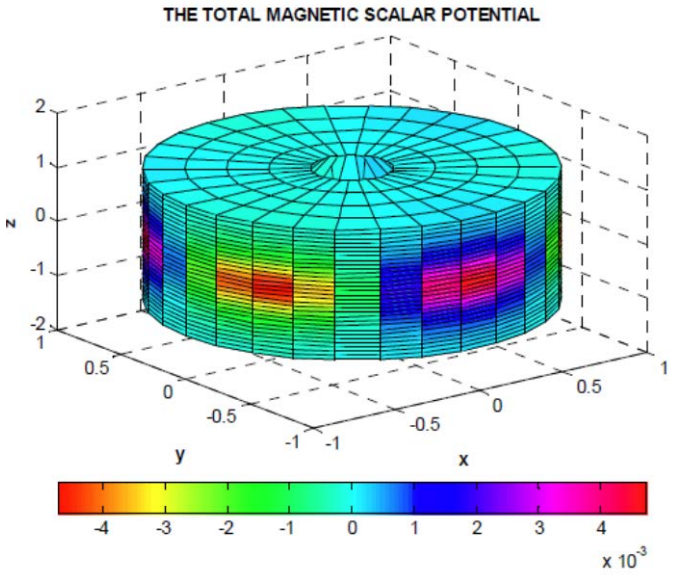

Figure 17: Scalar potential on cylinder outside the balanced 6 pole motor

In Figure (18), below, we show the *m = 2* contribution of the cylindrical decomposition of the potential on the observation cylinder. This is the term which would contain the spherical dipole (see Table 1) and since this is the case of the balanced motor, we expect this contribution to be very small. As can be seen from the Figure, the magnitude is several orders of magnitude down from the main field. We expect the main field to be dominated by the *m = 3* term as noted in the table. The *m = 3* term, shown in Figure (19), contains the spherical octupole or 6 radial pole distribution. It closely resembles the plot of Figure (17) which is the total potential.

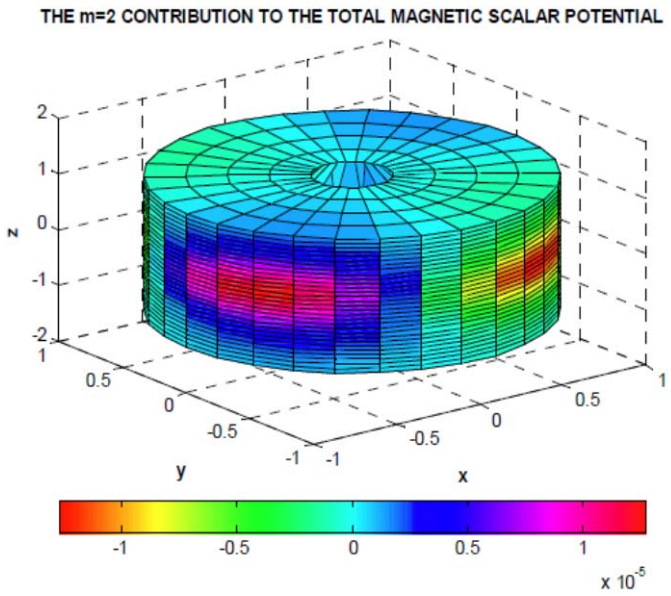

Figure 18: The m = 2 term of the Cylindrical Harmonic Distribution for the Case of a Balanced Motor.

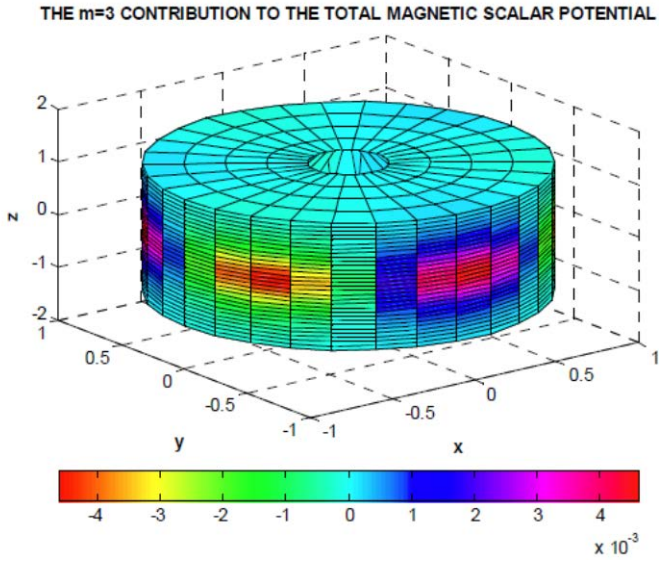

Figure 19: The m = 3 Term of the Cylindrical Expansion for the Balanced Case Showing the 6 Pole Distribution

The problem was then solved again and in this case one of the magnets was weakened as before. The plot of Figure (20) shows that instead of seeing the normal 6 pole distribution, the potential field is dominated by a dipole which appears as a result of the unbalance. The higher order terms fall off quickly so that even close to the source we see relatively few terms. The closer we can get to the machine frame, the more information we have.

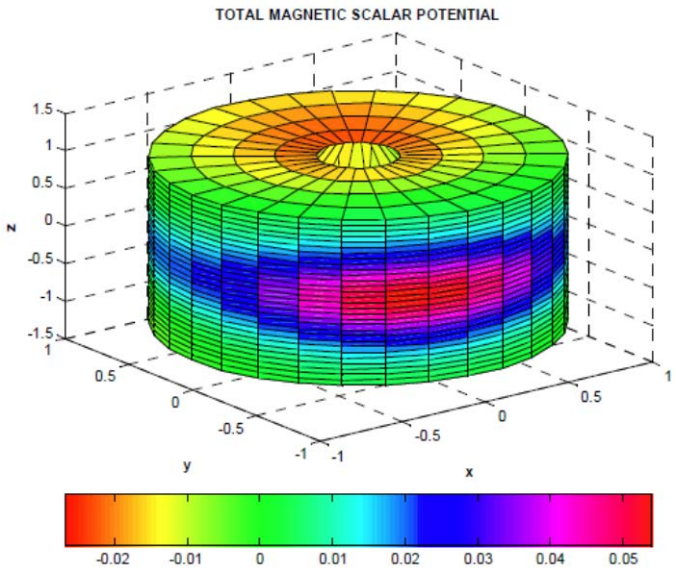

Figure 20: The Total Potential on an Exterior Cylinder for the Unbalanced Case.

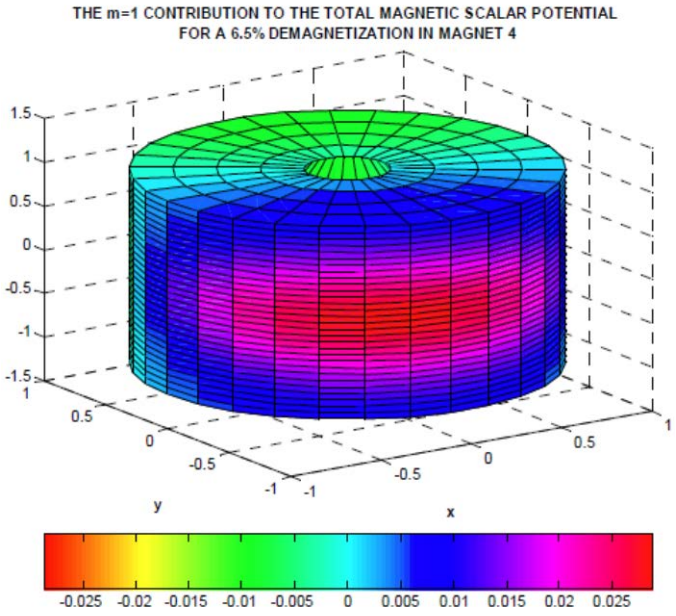

Figure 21: The *m = 1* Term for the Case of Unbalanced Magnets

In Figure (21) we see the *m = 1* term contribution in the cylindrical decompostion. Recall that this is the only possible term that could include a dipole and indeed the spherical dipole is apparent. This plot also resembles the total potential solution of Figure (20).

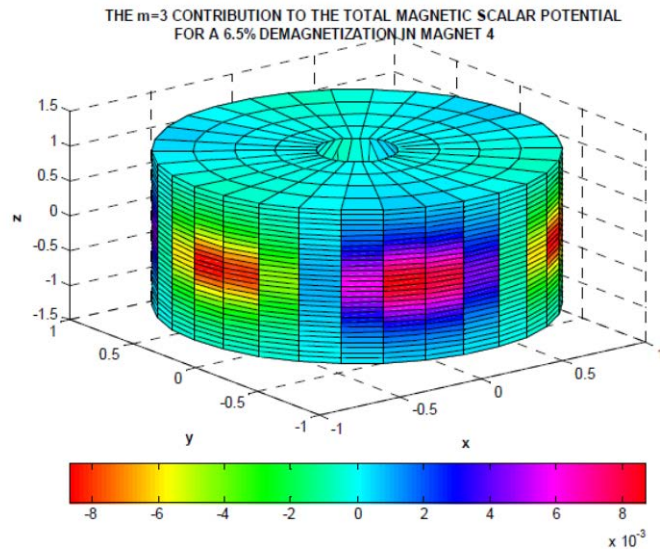

Figure 21: The *m = 3* Term of the Cylindrical Expansion for the Unbalanced Magnet Case

In Figure (21) we see the *m = 3* term of the expansion for the case of unbalanced magnets. This again is the term which contains the radial octupole. Comparing this to Figure (29) which is the *m = 3* term for the balanced case, we see that they are essentially the same. It is apparent that the cylindrical expansion yields as much physical insight as the spherical harmonics.

This analysis yields a simple illustration of how a demagnetized magnet can interrupt the symmetry that is associated with the balanced motor considered previously.

Other defects can also be treated in the same way. Consider the case where a fairly large axial off-set exists between the rotor and the stator, Figure (22) is a plot of the total magnetic scalar potential for the 6 pole motor with a 10 % axial off-set. In this case the magnets are balanced.

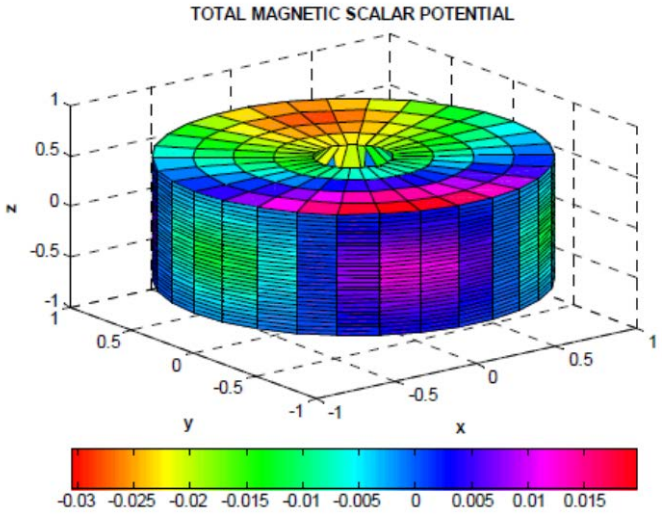

Figure 22: Total Magnetic Potential for the 6 Pole Motor with an Axial Offset.

The *m = 1* term for the axial offset case is shown in Figure (23). Comparing Figures (22) and (23), it is apparent that the distribution on the end of the cylinder due the offset is contained mostly in the *m = 1* term. Comparing the result of Figure (22) with the balanced or unbalanced magnet cases

which had no axial offset, we see that in those cases the potential on the top surface is fairly constant implying a low leakage field at the end of the machine. In Figure (24), which shows the *m = 3* contribution, we see a relatives weak distribution on the top surface but note that on the cylindrical side the 6 pole distribution is clearly present.

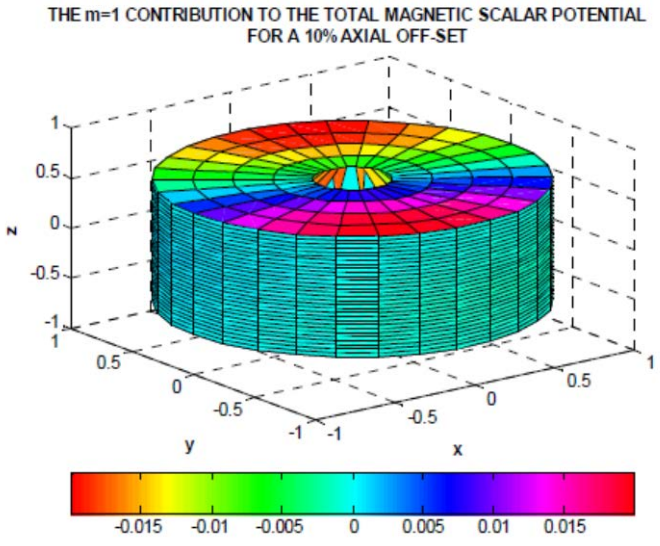

Figure 23: The *m = 1* Term of the Scalar Potential for the Axially Offset Motor

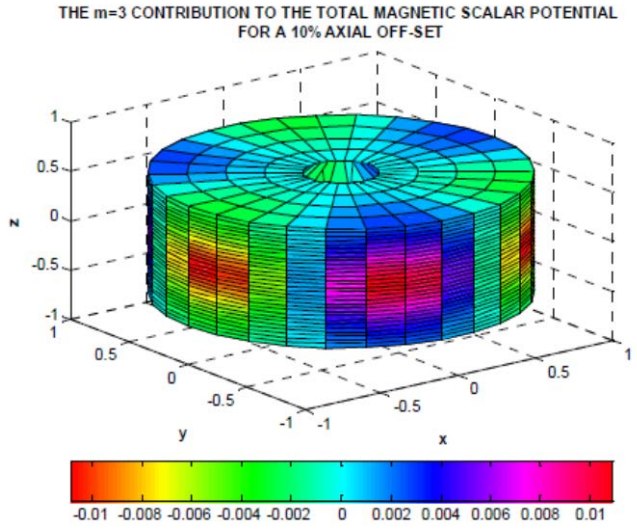

Figure 24: The *m = 3* term for the axially offset motor

One may notice that for the two unbalanced cases considered, a nontrivial dipole contribution appeared. This was not the case for the balanced motor. In fact, any motor imbalance such as magnet demagnetization, axial or radial offsets, etc., will interrupt the symmetry of the balanced motor. This loss of symmetry will ultimately be reflected in the low order multipole components.

Using this observation, the external leakage fields of an electric machine (or possibly other devices) can be used as a diagnostic tool. Reference [9] shows that defects in machines can be found by analysis of the magnetic signature. This is very attractive as it is completely non-invasive and can be done with the machines on-line. Different defects produce different harmonics in the far-field. For example, an unbalanced magnet will produce a dipole field as illustrated above. A shorted rotor turn in a 2 pole synchronous machine will produce a quadrupole. Depending on the number of poles in the machine, a static eccentricity will produce a stationary quadrupole, and so forth. These defects include misalignment, short circuits and eccentricities [41].

V. Conclusions

The toroidal expansion lends itself to a large class of problems. It is especially useful in geometries with large aspect ratios (length/diameter) as they enable accurate solutions close to the source. Since many solutions involve potential, these functions also have the advantage that derivatives can be found analytically, insuring smooth fields. These functions are very well behaved numerically and are evaluated as a summation which converges very quickly. Some example of recently solved problems using the Q functions are the gravitational potential of galaxies [21], charged finite disks [14], finite cylindrical current distributions, nonlinear pendulums, mutual inductance of coils, Helmholtz coils, to name a few.

This article has shown the viable application of these functions to a number of relevant problems. The Q functions are well-behaved and can be used in their own right or, as shown above, to post-process results found from numerical methods (see also Hameyer et. al [25]).

VI. References

[1] T. MacRobert, *Spherical Harmonics*. New York: Pergamon, 1967.

[2] P. M. Morse and H. Feshbach, *Methods of Theoretical Physics I&II*. New York: McGraw-Hill, 1953.

[3] E. T. Whittaker and G. N. Watson, *A Course of Modern Analysis*, 4th ed. Cambridge, U.K.: Cambridge Univ. Press, 1952.

[4] W. M. Hicks, "On toroidal functions," *Phil. Trans. R. Soc. Lond.*, vol 172, pp. 609–652, 1881.

[5] A. B. Bassett, "On toroidal functions," *Amer. J. Math.*, vol. 15, no. 4, pp. 287–302, Oct. 1893.

[6] A. Rotenberg, "The calculation of toroidal harmonics," *Math. Comput.*, vol. 14, no. 71, pp. 274–276, Jul. 1960.

[7] H. E. Fettis, "A new method for computing toroidal harmonics," *Math.Comput.*, vol. 24, no. 111, pp. 667–670, Jul. 1970.

[8] E. P. Furlani, *Permanent Magnet and Electromechanical Devices*. New York: Academic, 2001.

[9] Kwon, O-Mun, "The Analysis Of Effects Of Certain Asymmetries In Electrical Machines," Ph.D. dissertation, Rensselaer Polytechnic Institute, Troy NY, August 2003.

[10] Kwon, O-Mun, C.Surussavadee, M.V.K Chari, S.Salon, K.Sivasubramaniam,, "Analysis of the Far Field Permanent Magnet Motors and study of effects of geometric asymmetries and unbalance in magnet design," IEEE Transactions on Magnetics Vol. 40, No. 2, 435-442, 2004.

[11] Lebedev, N.N., Special Functions and Their Applications, Prentice-Hall, pp. 186-188, 1965.

[12] P.M. Morse, and H.Feshbach, Methods of Theoretical Physics, McGraw Hill, Parts I &II, p.744, pp.1301-1304, 1953.
[13] Schwab, A.J. Field Theory Concepts, Springer-Verlag, pp. 186-189, 1988.
[14] Selvaggi, J, "Multipole Analysis of Circular Cylindrical Magnetic Systems, Ph.D. dissertation, Rensselaer Polytechnic Institute, Troy NY, May 2005.
[15] Selvaggi, J., S. Salon, O-Mun Kwon, M.V.K Chari, "Calculating the External Magnetic Field from Permanent Magnets in Permanent-Magnet Motors-An Alternative Method," IEEE Transactions on Magnetics, Vol. 40, No. 5, pp. 3278- 3285, September 2004.
[16] Smythe, W.R., Static and Dynamic Electricity, McGraw-Hill, 3rd ed., p. 204, 1968.
[17] Snow, C., Formulas for Computing Capacitance and Inductance, National Bureau of Standards Circular 544, pp. 13-17, September 1, 1954.
[18] Snow, C., Hypergeometric and Legendre Functions with Applications to Integral Equations of Potential Theory, National Bureau Of Standards Applied Mathematics Series 19, U.S. Department of Commerce, pp. 228-252, May 1, 1952.
[19] Snow, C., Potential Problems and Capacitance for a Conductor Bounded by Two Intersecting Spheres, U.S. Department of Commerce NBS, Research Paper RP2032, Vol. 43, pp. 377-407, October 1949.
[20] Stratton, J. A, Electromagnetic Theory, McGraw-Hill Book Company, pp. 241- 242, 1941.
[21] Jerry P Selvaggi, Sheppard Salon, M V K Chari, "The Newtonian force experienced by a point mass near a finite cylindrical source", Class. Quantum Grav.25, (2008)
[22] E.P. Furlani, S. Reznik, and W. Janson, "A Three-Dimensional Field Solution for Bipolar Cylinders," IEEE Transactions of Magnetics, Vol. 30, No. 5, September 1994
[23] L. K. Urankar, "Vector Potential and Magnetic Field of Current-Carrying Finite Arc Segment in Analytical Form, Part I: Filament Approximation," IEEE Transactions of Magnetics, Vol. Mag-16, No. 5, September 1980.
[24] E.W. Hobson, On Green's Function for a Circular Disk, with applications to Electrostatic Problems, Transactions of the Cambridge Philosophical Society, Vol. 18, 1900.
[24] E.W. Hobson, On Green's Function for a Circular Disk, with applications to Electrostatic Problems, Transactions of the Cambridge Philosophical Society, Vol. 18, 1900
[25] K.Hameyer, R.Mertens, U.Pahner, R.Belmans: "New technique to enhance the accuracy of 2-D/3-D field quantities and forces obtained by standard finite-element solutions", *IEE Journal of Science, Measurement and Technology*, Vol.145, No.2, March 1998, pp.67-75.
[26] C. Snow, "Magnetic fields of cylindrical coils and annular coils," *Natl.Bur. Stand.*, ser. Applied Mathematics, vol. 38, pp. 1–29, 1953.
[27] H. E. Fettis, "A new method for computing toroidal harmonics," *Math.Comput.*, vol. 24, no. 111, pp. 667–670, Jul. 1970.
[28] H. S. Cohl and J. E. Tohline, "A compact cylindrical green's function expansion for the solution of potential problems" *Astrophys. J.*, vol. 527, pp. 86–101, Dec. 1999.
[29] H. S. Cohl, A. R. P. Rau, J. E. Tohline, D. A. Browne, J. E. Cazes,and E. I. Barnes, "Useful alternative to the multipole expansion of 1/r potentials," *Phys. Rev. A*, vol. 64, pp. 052509-1–5, 2001.
[30] M. Abramowitz and I. Stegun, *Handbook of Mathematical Functions*. New York: Dover, 1972.
[31] R.A. Schill, "General Relation for the Vector Magnetic Field of a Circular Current Loop: A Closer Look," IEEE Transactions on Magnetics, Vol. 39, No. 2, March 2003.
[32] S. Babic, C. Akyel, and J. Salon, "New Procedures for Calculating the Mutual Inductance of the System: Filamentary Circular Coil-Massive Circular Solenoid," IEEE Transactions of Magnetics, Vol. 39, No. 3, May 2003.
[33] D.J. Craik and A.J. Harrison, "Comparative magnetostatic analyses of axisymmetric systems," J. Phys. D: Appl. Phys., Vol. 7, 1974.
[34] S. Babic, S. Salon, "The Mutual Inductance of Two Thin Coaxial Disk Coils in Air," IEEE Transactions of Magnetics, Vol. 40, No. 2, March 2004.
[35] C.M. Butler, "Capacitance of a finite-length conducting cylindrical tube," Journal of Applied Physics, Vol. 51, No. 11, November 1980
[36] T.T. Ferguson and R.H. Duncan, "Charged Cylindrical Tube," Journal of Applied Physics, Vol. 32, No. 7, July 1961
[37] G.A. Estevez, "Solution to a classical problem in electrostatics in Legendre polynomials expansion," American Journal of Physics, Vol. 56, No. 12, December 1988
[38] P. Moon and D.E. Spencer, "Separability in a Class of Coordinate Systems," Journal of Franklin Institute, September 1952. 98
[39] P. Moon and D.E. Spencer, "Some Coordinate Systems Associated with Elliptic Functions," Journal of Franklin Institute, June 1953.
[40] P. Moon and D.E. Spencer, "Cylindrical and Rotational Coordinate Systems," Journal of Franklin Institute, October 1951.
[41] US Patent GB2457590: O-Mun Kwon, Sameh R Salem, Sheppard Salon, Madabushi Venkatakrishnama Chari: Methods and systems for detecting abnormalities in rotating machinery. Aug, 26 2009

ACKNOWLEDGEMENTS

The author would like to acknowledge the advice and suggestions of Dr. M.V.K. Chari. His comments helped to improve and clarify this article. This article also heavily relies on the PhD work at Rensselaer Polytechnic Institute of O-Mun Kwon, Kiruba Haran and Jerry Selvaggi who first used the toroidal functions for this purpose.

AUTHOR'S NAME AND AFFILIATION

Sheppard Salon, salons@rpi.edu is an Emeritus Professor at Rensselaer Polytechnic Institute in Troy New York. He is in the Department of Electrical, Computer and Systems Engineering.